Available online at www.sciencedirect.com
ScienceDirect
Journal of Power Sources 162 (2006) 94–104
JOURNAL OF POWER SOURCES
www.elsevier.com/locate/jpowsour

Effect of flow pattern of gas and cooling water on relative humidity distribution in polymer electrolyte fuel cell

Gen Inoue [a,*], Takashi Yoshimoto [a], Yosuke Matsukuma [a], Masaki Minemoto [a], Hideki Itoh [b], Shigeru Tsurumaki [b]

[a] *Department of Chemical Engineering, Faculty of Engineering, Kyushu University Motooka, Nishi-ku, Fukuoka 819-0395, Japan*
[b] *Mitsubishi Heavy Industries, Ltd., Kan-on-shin-machi, Nishi-ku, Hiroshima 733-8553, Japan*

Received 27 April 2006; received in revised form 3 July 2006; accepted 5 July 2006
Available online 22 September 2006

Abstract

In actual size of polymer electrolyte fuel cell stack with heat management of cooling water, relative humidity distribution was calculated under various kinds of operating conditions and various shapes of gas channel with numerical analysis. And the optimal separator shape and the optimal flow pattern of gas and cooling water that make the relative humidity higher and more uniform and that lead to the improvement of cell durability were examined under each operating condition. As a result, the effects of humidify temperature, the temperature of cooling water at an outlet and the average current density on humidity distribution which was affected by vapor concentration and gas temperature were examined and it was found that the optimal combination of flow pattern of gas and cooling water was the same under each operating condition. As regards the operating condition in this paper, the relative humidity is the highest and the most uniform in the following cases: gas flow pattern is counter, the cooling water is synchronized with cathode gas flow and the ordinary serpentine separator with 1.0 mm depth channels is used in cathode and anode sides. However, it is found that it is possible to occur the flooding in such cases.

Keywords: PEFC; Numerical analysis; Relative humidity distribution cooling water; Flooding

1. Introduction

Polymer electrolyte fuel cell (PEFC) is a promising new clean and efficient generator, however, it needs to be improved its performance for general practical use. Recently, many studies have been reported about improvement of the output performance and the durability of PEFC. In these studies, it was reported that the degradation of the MEA caused a drop of cell voltage and a break in the electrolyte membrane. Though the degradation mechanism has not been investigated in detail yet, it is thought that peroxide radical attack is responsible for this degradation phenomenon. It was reported that this degradation was accelerated under low humidity condition [1–3]. As concerns the basis of this experimental result, it is effective to increase the average relative humidity and to make its distribution uniform in a cell in order to improve the PEFC durability related to the degradation of the MEA because a part of low humidity is reduced. On the other hand, when the humidity becomes high to excess, vapor is condensed into liquid droplets. As a result, the droplets block the diffusion of reactant gas in gas diffusion layer (GDL) and the flow of the supplied gas in gas channels. Concerning such flooding phenomena, there have been some studies which examine them by experiments or numerical analysis. The investigation of degradation mechanism by flooding and the examination of improvement of discharging liquid water have been reported [4–9]. It is also effective to decrease the average relative humidity and to make its distribution uniform in a cell in order to improve the PEFC durability related to the flooding because the areas of high humidity are reduced.

Consequently, the relative humidity distribution must be uniform and appropriate value, which should not be too high or too low, from the both viewpoints of the degradation of MEA and flooding. It is important to examine the relative humidity distribution in PEFC for improvement of cell performance and

* Corresponding author. Tel.: +81 92 802 2765; fax: +81 92 802 2785.
E-mail address: ginoue@chem-eng.kyushu-u.ac.jp (G. Inoue).

0378-7753/$ – see front matter © 2006 Elsevier B.V. All rights reserved.
doi:10.1016/j.jpowsour.2006.07.018

Nomenclature

b_c	condensation rate constant ($1\ s^{-1}$)
C_j	molar concentration of species j ($mol\ m^{-3}$)
$C_{j(n)}$	molar concentration of species j in next channel of n direction ($mol\ m^{-3}$)
C_p	specific heat at constant pressure ($J\ kg^{-1}\ K^{-1}$)
$C^e_{O_2}$	oxygen concentration at catalyst layer ($mol\ m^{-3}$)
$C^{ref}_{O_2}$	reference oxygen concentration ($mol\ m^{-3}$)
D_j	diffusion coefficient of species j ($m^2\ s^{-1}$)
D^{eff}_j	effective diffusion coefficient of species j ($m^2\ s^{-1}$)
E	electromotive force (V)
$E_{\Delta H}$	the value of reduction change of water enthalpy to voltage (V)
F	Faraday's constant ($96485C\ mol^{-1}$)
h	heat transfer coefficient of gas ($J\ m^{-2}\ s^{-1}\ K^{-1}$)
h^w	heat transfer coefficient of cooling water ($J\ m^{-2}\ s^{-1}\ K^{-1}$)
H_{GDL}	length of GDL gas flow area (m)
ΔH_{H_2O}	change of water enthalpy between vapor and liquid ($J\ mol^{-1}$)
i	current density ($A\ m^{-2}$)
i_{O_2}	oxygen exchange current density ($A\ m^{-2}$)
k	thermal conductivity of solid phase ($J\ m^{-1}\ s^{-1}\ K^{-1}$)
k_p	permeability of GDL (m^2)
k^{sep}	thermal conductivity of separator ($J\ m^{-1}\ s^{-1}\ K^{-1}$)
$l_{d,g}$	gas channel depth (m)
l_{GDL}	GDL thickness (m)
l^S	thickness of solid phase (m)
l^{sep}	separator thickness between cooling water and gas phase (m)
M_j	molecular weight of species j ($kg\ mol^{-1}$)
p	pressure (Pa)
p_n	pressure in next channel of n direction (Pa)
$P_{H_2O,sat}$	saturated vapor pressure in stream (Pa)
Q_b	all gas flow rate through GDL per unit volume to next channel ($1\ s^{-1}$)
$Q_{b(n)}$	flow rate through GDL per unit volume to next channel of n direction ($1\ s^{-1}$)
$Q_{b(n,in)}$	inflow rate through GDL per unit volume from next channel of n direction ($1\ s^{-1}$)
$Q_{b(n,out)}$	outflow rate through GDL per unit volume to next channel of n direction ($1\ s^{-1}$)
q_1	heat flux from solid phase to gas phase ($J\ m^{-2}\ s^{-1}$)
q_2	heat flux from cooling water to gas phase ($J\ m^{-2}\ s^{-1}$)
q^s_3	heat value generated by reaction ($J\ m^{-2}\ s^{-1}$)
q^s_4	heat flux from gas phase to solid phase ($J\ m^{-2}\ s^{-1}$)
q^s_5	heat flux from cooling water to solid phase ($J\ m^{-2}\ s^{-1}$)
q^s_6	latent heat value of condensation ($J\ m^{-2}\ s^{-1}$)
q^w_1	heat flux from both side gas to cooling water ($J\ m^{-2}\ s^{-1}$)
q^w_2	heat flux from solid phase to cooling water ($J\ m^{-2}\ s^{-1}$)
R	gas constant ($8.314\ J\ mol^{-1}K^{-1}$))
R_{rea}	all reaction rate ($1\ s^{-1}$)
r_j	molar flux of species j ($mol\ m^{-2}\ s^{-1}$))
R_{ohm}	resistance of proton transfer through electrolyte membrane ($\Omega \cdot m^2$)
Re	Reynolds number defined in Table 1
Sc	Schmitt number defined in Table 1
Sh	Sherwood number defined in Table 1
t	time (s)
T	gas phase temperature (K)
T_n	gas temperature in next channel of n direction (K)
T^s	solid phase temperature (K)
T^w	cooling water temperature (K)
U	average gas velocity in GDL of x direction ($m\ s^{-1}$)
U_T	overall heat transfer coefficient between gas and cooling water ($J\ m^{-2}\ s^{-1}\ K^{-1}$)
U^s_T	overall heat transfer coefficient between cooling water and solid phase ($J\ m^{-2}\ s^{-1}K^{-1}$)
v	flow velocity ($m\ s^{-1}$)
V	operation voltage (V)
w_C	channel width (m)
w_L	land width (m)
x	x direction (m)

Greek letters

α	net water transfer coefficient
α_t	transfer coefficient
β	parameter in oxygen mass transfer model shown in Table 1
ε	effective porosity of GDL
γ	variable defined in Table 1 ($A\ m\ mol^{-1}$)
λ	parameter defined in Table 1
μ	viscosity of mixture gas (Pa·s)
ρ	density of mixture gas ($kg\ m^{-3}$)
ω	parameter in oxygen mass transfer model shown in Table 1

Subscripts

H_2O	water
$H_2O(l)$	liquid water
$H_2O(v)$	vapor water
j	species j
N_2	nitrogen
O_2	oxygen
x	x direction

Superscripts

a	anode
c	cathode
channel	channel
e	electrode

eff	effective
k	anode or cathode
s	solid phase
sep	separator

numerical analysis is one of the tools to examine the humidity distribution under various operating conditions and various shapes. In our past research [10], author developed a reaction and thermal flow analysis model in PEFC stack including the thermal management by cooling water. The relative humidity distribution was examined under sixteen conditions about the flow pattern of gas and cooling water and about channel shape. Moreover, the optimal flow pattern of gas and cooling water and the optimal shape of channel were examined to make the relative humidity distribution more uniform with this model. However, as this result was obtained under only one operating condition, it was thought that the different results might be obtained under different operating conditions (average current density, humidity temperature, temperature of cooling water). In this study, with the same PEFC analysis model including the effect of cooling water as our past model [10], the relative humidity distribution was calculated under various operating conditions about four

Table 1
Basic equations for this study

Continuity in channel $\dfrac{\partial v^k}{\partial x} = -R^k_{\mathrm{rea}} - Q^k_b$

Motion in channel $\rho^k \dfrac{\mathrm{D}v^k}{\mathrm{D}t} = -\nabla p^k + \rho^k v^k (R^k_{\mathrm{rea}} + Q^k_b) - 12\mu^k \left(\dfrac{1}{(l^k_{\mathrm{d,g}})^2} + \dfrac{1}{(w^k_{\mathrm{C}})^2} \right) v^k$

Mass balance in channel $\dfrac{\mathrm{D}C^k_j}{\mathrm{D}t} = -\dfrac{r^k_j}{l^k_{\mathrm{d,g}}} + C^k_j (R^k_{\mathrm{rea}} + Q^k_b) + \sum_n C^k_{j(n)} Q^k_{b(n,\mathrm{in})} - \sum_n C^k_j Q^k_{b(n,\mathrm{out})}$

Energy in channel $\dfrac{\mathrm{D}T^k}{\mathrm{D}t} = \dfrac{q^k_1 + q^k_2}{\rho^k C^k_p l^k_{\mathrm{d,g}}} + T^k (R^k_{\mathrm{rea}} + Q^k_b) + \sum_n T^k_n Q^k_{b(n,\mathrm{in})} - \sum_n T^k Q^k_{b(n,\mathrm{out})}$

Energy in MEA and GDL $\rho^{\mathrm{s}} C^{\mathrm{s}}_p \dfrac{\partial T^{\mathrm{s}}}{\partial t} = k^{\mathrm{s}} \nabla^2 T^{\mathrm{s}} + \dfrac{q^{\mathrm{s}}_3 + q^{\mathrm{s}}_4 + q^{\mathrm{s}}_5 + q^{\mathrm{s}}_6}{l^s}$

Energy of cooling water $\dfrac{\mathrm{D}T^w}{\mathrm{D}t} = \dfrac{q^w_1 + q^w_2}{\rho^w C^w_p l^w}$

Gas flow rate through GDL $Q^k_{b(n)} = \dfrac{k_p}{\mu^k} \dfrac{l^k_{\mathrm{GDL}}}{l^k_{\mathrm{d,g}} w^k_{\mathrm{C}} w^k_{\mathrm{L}}} (p^k - p^k_n) \quad Q^k_b = \sum_n Q^k_{b(n)}$

Reaction rate
$$r^{\mathrm{a}}_{\mathrm{H_2}} = \frac{i}{2F}, \quad r^{\mathrm{a}}_{\mathrm{H_2O}(v)} = \alpha \frac{i}{F} + l^{\mathrm{a}}_{\mathrm{d,g}} b_{\mathrm{c}} \left(C^{\mathrm{a}}_{\mathrm{H_2O}(v)} - \frac{P^{\mathrm{a}}_{\mathrm{H_2O,sat}}}{RT^a} \right), \quad r^{\mathrm{a}}_{\mathrm{N_2}} = 0$$
$$r^{\mathrm{c}}_{\mathrm{O_2}} = \frac{i}{4F}, \quad r^{\mathrm{c}}_{\mathrm{H_2O}(v)} = -(1+2\alpha)\frac{i}{2F} + l^{\mathrm{c}}_{\mathrm{d,g}} b_{\mathrm{c}} \left(C^{\mathrm{c}}_{\mathrm{H_2O}(v)} - \frac{P^{\mathrm{c}}_{\mathrm{H_2O,sat}}}{RT^{\mathrm{c}}} \right), \quad r^{\mathrm{c}}_{\mathrm{N_2}} = 0$$
$$r^{\mathrm{a}}_{\mathrm{H_2O}(l)} = -l^{\mathrm{a}}_{\mathrm{d,g}} b_{\mathrm{c}} \left(C^{\mathrm{a}}_{\mathrm{H_2O}(v)} - \frac{P^{\mathrm{a}}_{\mathrm{H_2O,sat}}}{RT^{\mathrm{a}}} \right), \quad r^{\mathrm{c}}_{\mathrm{H_2O}(l)} = -l^{\mathrm{c}}_{\mathrm{d,g}} b_{\mathrm{c}} \left(C^{\mathrm{c}}_{\mathrm{H_2O}(v)} - \frac{P^{\mathrm{c}}_{\mathrm{H_2O,sat}}}{RT^{\mathrm{c}}} \right)$$
$$R^k_{\mathrm{rea}} = \frac{1}{l^k_{\mathrm{d,g}} \rho^k} \sum_j M_j r^k_j$$

Heat flux
$$q^k_1 = h^k (T^{\mathrm{s}} - T^k), \quad q^k_2 = U^k_T (T^w - T^k), \quad q^{\mathrm{s}}_3 = (E_{\Delta H} - V) i$$
$$q^{\mathrm{s}}_4 = h^{\mathrm{a}} (T^{\mathrm{a}} - T^{\mathrm{s}}) + h^{\mathrm{c}} (T^{\mathrm{c}} - T^{\mathrm{s}}), \quad q^{\mathrm{s}}_5 = 2U^{\mathrm{s}}_T (T^w - T^{\mathrm{s}})$$
$$q^{\mathrm{s}}_6 = -\Delta H_{\mathrm{H_2O}} (r^{\mathrm{a}}_{\mathrm{H_2O}(l)} + r^{\mathrm{c}}_{\mathrm{H_2O}(l)})$$
$$q^w_1 = U^{\mathrm{a}}_T (T^{\mathrm{a}} - T^w) + U^{\mathrm{c}}_T (T^{\mathrm{c}} - T^w), \quad q^w_2 = 2U^{\mathrm{s}}_T (T^{\mathrm{s}} - T^w)$$
$$U^k_T = \frac{1}{\dfrac{1}{h^k} + \dfrac{l^{\mathrm{sep}}}{k^{\mathrm{sep}}} + \dfrac{1}{h^w}}, \quad U^{\mathrm{s}}_T = \frac{1}{\dfrac{l^{\mathrm{sep}} + l^k_{\mathrm{d,g}}}{k^{\mathrm{sep}}} + \dfrac{1}{h^w}}$$

Current density $V = E - \dfrac{RT}{\alpha_t 2F} \ln \left[\dfrac{i\, C^{\mathrm{ref}}_{\mathrm{O_2}}}{i_{\mathrm{O_2}}\, C^e_{\mathrm{O_2}}} \right] - R_{\mathrm{ohm}} i \quad \gamma = \dfrac{i_{\mathrm{O_2}}}{C^{\mathrm{ref}}_{\mathrm{O_2}}}$

Oxygen mass transfer in GDL
(upstream) $\mathrm{Sh} = \beta + \lambda\, \mathrm{Re}^{0.5}\, \mathrm{Sc}^{0.8}$
(downstream) $\mathrm{Sh} = \beta + \lambda (Re - \omega)^{0.5}\, \mathrm{Sc}^{0.5}$

$$\mathrm{Sh} = \frac{i}{4F} \frac{l_{\mathrm{GDL}}}{D^{\mathrm{eff}}_{\mathrm{O_2}} (C^{\mathrm{channel}}_{\mathrm{O_2}} - C^e_{\mathrm{O_2}})} \quad Re = \frac{l_{\mathrm{GDL}} \rho U}{\mu} \quad \mathrm{Sc} = \frac{\mu}{\rho D^{\mathrm{eff}}_{\mathrm{O_2}}}$$
$$\lambda = \frac{1}{2} \sqrt{\frac{l_{\mathrm{GDL}}}{\pi H_{\mathrm{GDL}}}} \quad D^{\mathrm{eff}}_j = \varepsilon D_j$$

combinations of flow pattern and channel shape which were considered the influences in [10]. The optimal flow pattern of gas and cooling water and the optimal shape of channel which lead to improvement of PEFC performance were examined from the viewpoints of degradation of MEA and flooding.

2. Numerical analysis model

In this study, the PEFC numerical analysis model that had been developed in our former study [10] was used. This numerical analysis model was developed with the following assumptions.

(1) The gas flow rate at the inlet in each channel is uniform.
(2) The volume of liquid water is ignored and the water moves with the gas.
(3) The reduction of the reaction area caused by flooding of electrode is ignored and it is also ignored that liquid water prevents the diffusion.
(4) Fluid is incompressible Newtonian fluid and ideal gas. The flow condition is laminar flow. The gas properties are constant.
(5) Heat transfer between separator and gas is ignored. But heat transfer among gas phase, solid phase and cooling water is included.
(6) Cell voltage is uniform and constant.
(7) Only resistance overvoltage and water transfer in membrane include the influence of temperature.
(8) In membrane, ionic conductivity, electro osmosis coefficient and water effective diffusion coefficient that depend on membrane humidity are determined by water activity in anode side.
(9) The crossover of gases through membrane is disregarded.
(10) The permeability of GDL is constant and uniform.

The assumptions 2 and 3 are not appropriate under the case of excessive flooding conditions. However, it was assumed that excessive flooding was not caused in this study and it was thought that the influence of water in channels and GDL on the cell performance was very small.

The basic equations and the schematic analysis model are shown in Table 1, respectively. The derivation of these basic equations was shown in references [10,11], but it was omitted in this study. In our former study, the numerical analysis model including the effect of thermal management with cooling water was developed. As compared with the back plate of which the temperature is constant, the effect of cooling water was changed by the flow pattern and the flow rate. The heat transfer from MEA, anode gas and cathode gas were combined with the one-dimensional energy equation and the temperature of cooling water was calculated along the channels. When the flow, the concentration and the temperature of anode and cathode gas were calculated, the quasi-two-dimensional model including the effect of gas flow through GDL was used. The temperature of MEA was calculated with the two-dimensional energy equation and the overvoltage equation including the characteristic of mass transfer in GDL, which was developed in reference [11], was used in order to calculate the current density. Those variables were calculated until they became stationary state and the relative error of all mass and energy balances became less than 1%. In this study, gas flow rate was automatically set by the utilization and current density and the flow rate of cooling water was also automatically set by the temperature at the inlet and the outlet.

3. Results and discussions

The calculation conditions are shown in Table 2. In this calculation, the average current density, the temperature of cooling water at the output and the humidity temperature were set under two kinds of condition. Table 3 shows each combination of these values and condition numbers. In this study, the operating condition was decided on the assumption that excessive flooding is not caused. To put it concretely, the temperature of cooling water was set higher than that of humidifier so that vapor partial pressure could not be much higher than saturated vapor pressure, if the generated water was added. On the basis of the result of our past study [10], calculations were carried out under four kinds of flowing conditions about gas and cooling water and the relative humidity was uniform or not low comparatively under these four conditions. The shapes of gas channel are shown in Fig. 1. The electrode area is 225 cm^2 (a square with side 15 cm long) and channel width and land width are 1 mm.

Table 2
Operating condition and shape of cell

Pressure (MPa)	0.1
Inlet gas temperature (°C)	70
Inlet temperature of cooling water (°C)	70
Outlet temperature of cooling water (°C)	75, 80
Humidify temperature (°C)	65, 55
Inlet gas composition	
Anode	H_2:N_2 = 75:25
Cathode	O_2: N_2 = 21:79
H_2 utilization (%)	70
O_2 utilization (%)	40
Thickness of membrane (μm)	30
Size of catalyst layer (cm^2)	225
GDL thickness (μm)	300
Channel width (mm)	1
Channel depth (mm)	1, 0.5
Land width (mm)	1
GDL permeability (m^2)	2.5×10^{-11}
Electromotive force (V)	1.23
Average current density (A cm^{-2})	0.4, 0.8

Table 3
Combination of operating condition

No.	Average current density (A cm^{-2})	Humidify temperature (°C)	Outlet temperature of cooling water (°C)
Condition 1	0.4	65	75
Condition 2	0.4	65	80
Condition 3	0.4	55	75
Condition 4	0.8	65	75

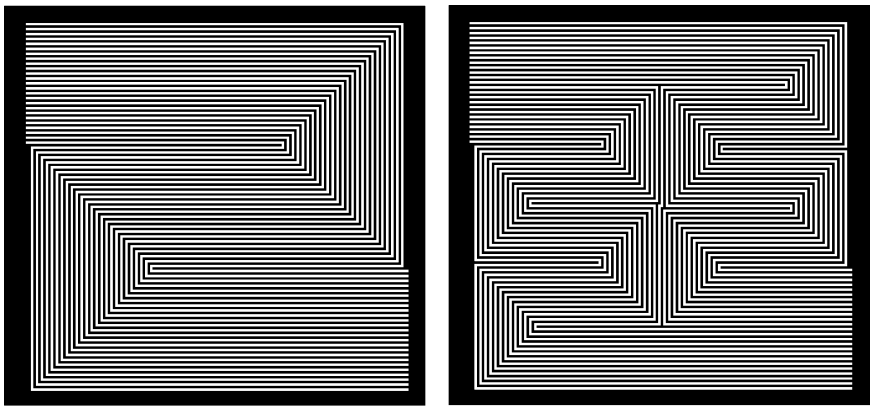

(A) (B)

Fig. 1. Separator shape: (A) is the ordinary serpentine separator; (B) is the distributed serpentine separator.

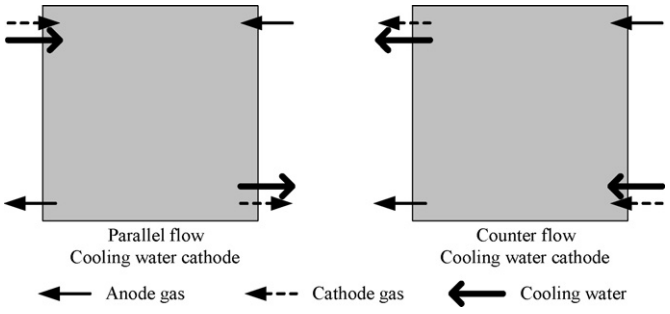

Fig. 2. The flow pattern of gas and cooling water.

A is the ordinary serpentine separator; B is the distributed serpentine separator and both separators have 25 channels. The shape of cooling water channel is the same as that of anode gas channel or cathode gas channel. Fig. 2 shows the flow pattern of gas and cooling water. And the calculation results of two kinds of channel depth (1.0 and 0.5 mm) were compared. Table 4 shows the combination of separator shapes and flow pattern.

Fig. 3 shows the cell voltage and the average relative humidity (RH) of anode and cathode under each condition and the results are shown in the case that channel depth was 1.0 and 0.5 mm. In this figure, it is confirmed that the average relative humidity of anode and cathode gas was less than 100% under all conditions and that there is not excessive flooding condition. It was found that the anode and cathode average humidity in the case of cooling water at high temperature (Condition 2) were lower than that of other conditions. Similarly, in the case of the humidity at low temperature (Condition 3), they were lower than that of other conditions. In Fig. 3(a–c), cell voltages were almost equal to others under each condition in the case that the average current density was 0.4 A cm^{-2}, on the other hand, in Fig. 3(d), cell voltage was affected by channel depth when the average current density was 0.8 A cm^{-2}. With shallow gas channels, pressure drop in a gas channel increased and differential pressure between adjoining channels increased. As a result, the gas flow rate through GDL increased and the oxygen mass transfer rate to the surface of electrode raised. Therefore cell voltage increased in the case of shallow gas channel. It was thought that the effect of the depth of gas channel was more remarkable under enough humidity condition with high current density because the oxygen mass transfer in GDL was more dominant than the proton mass transfer in membrane. Next, it was found that the anode average humidity on high current density (Condition 4) was lower than that on low current density (Conditions 1–3) and that the cathode average humidity was not affected by current density and it was equal to each other under each condition. As the utilization was set constant in this paper, cathode relative humidity was almost constant even if the amount of generated water increased under high current density condition. However, it was thought that anode gas became drier because the amount of water transfer in membrane from anode to cathode by electro-osmosis effect increased under high current density condition. Moreover, it was confirmed that anode and the cathode average relative humidity was not affected by the depth of channel under each condition and that the average relative humidity of counter flow (Nos. 2, 4) was higher than that of parallel flow (Nos. 1, 3), as well as the result in our past paper [10].

Anode relative humidity distributions under each condition are shown in Fig. 4. In Fig. 4(a), it was confirmed that the humidity at turning areas of channels was high with shallow channels. As the channels are shallow, the gas flow rate through GDL increases. At the turning areas of channels, the gas flow rate along the channel particularly decreases because the differential pressure between adjoining channels is larger than that of other areas. As a result, the effect of water transfer from cathode by back-diffusion is relatively larger than that of vapor convention by gas flow and the anode gas at these areas become humid. By contrast, the anode gas becomes dry at the areas where the gas flow rate along the channels is higher than other areas. The

Table 4
Combination of separator shape and flow pattern

No.	Anode separator	Cathode separator	Flow pattern	Cooling water pattern	Channel depth (mm)
1	A	A	Parallel	Cathode	1.0 or 0.5
2	A	A	Counter	Cathode	1.0 or 0.5
3	A	B	Parallel	Cathode	1.0 or 0.5
4	A	B	Counter	Cathode	1.0 or 0.5

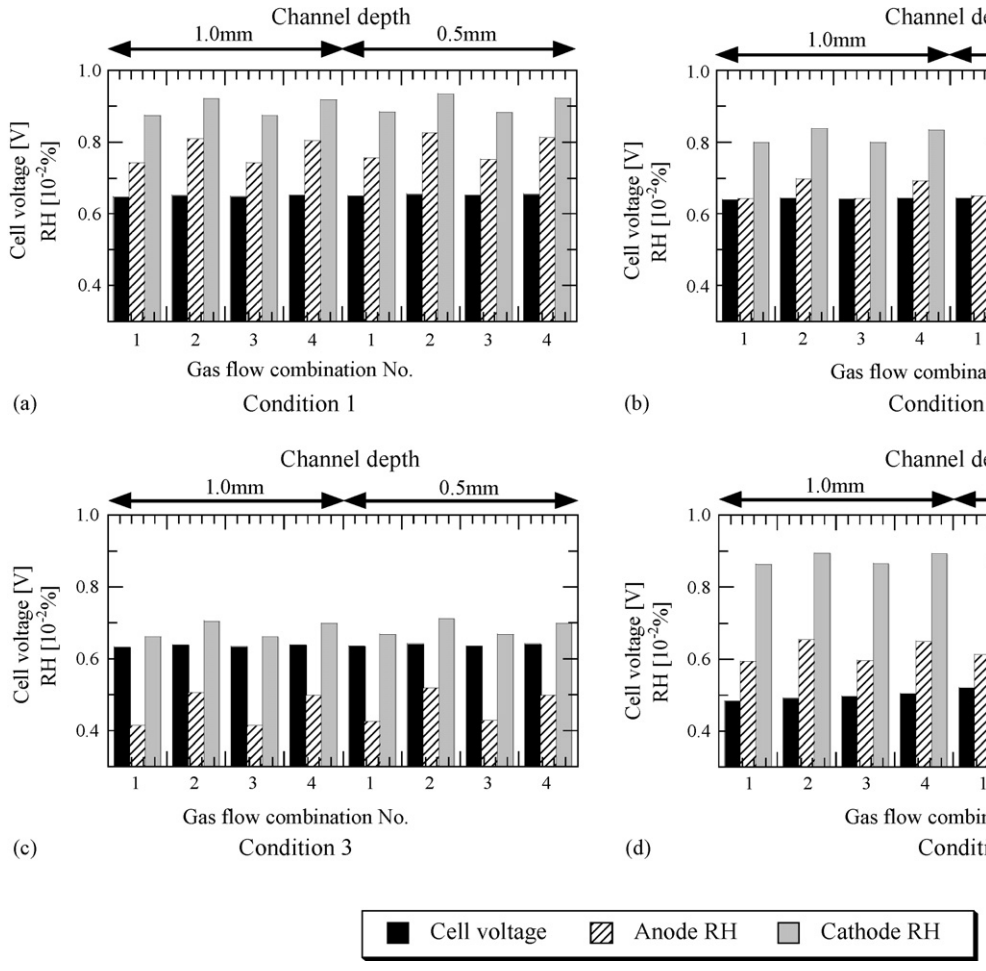

Fig. 3. Cell voltage and the average relative humidity under each operating condition.

results mentioned above could be confirmed under other operating conditions. Next, it was found that the humidity distribution of counter flow (Nos. 2, 4) was more uniform than that of parallel flow (Nos. 1, 3). As compared with the results of ordinary serpentine separator (Nos. 1, 2), it was also found that the humidity at turning areas with distributed serpentine separator was lower because the gas flow through GDL was reduced in this separator (Nos. 3, 4) and that the trend became remarkable in the case of shallow channels. However, it cannot be positively declared that the distributed serpentine separator was effective in the uniform humidity distribution because the overall humidity distribution with the distributed serpentine separator was complex. Though author explained that the distributed serpentine separator was effective in the improvement of output performance in the case of high gas flow rate and the low utilization in our past papers [11,12], it was thought that this separator was not effective in the decrease of membrane degradation caused by humidity distribution because the cell voltage was not improved very much and the humidity distribution was not uniform in the case of low gas flow rate under such operating conditions of this paper. In Fig. 4(a) and (b), as compared with Condition 1, it was found that the anode humidity at cathode down stream area decreased and the humidity distribution was more uniform in the case of the high temperature of cooling water at the outlet (Condition 2). It was thought to be caused because of the followings: Anode vapor concentration at the area corresponded to cathode down stream tends to increase by the back diffusion from cathode side. However, as the cooling water was supplied along the cathode gas flow, gas temperature on both sides at cathode downstream area became high. And as the cooling water was hot at the outlet, anode relative humidity decreased. In Fig. 4(a) and (c), as compared with Condition 1, it was found that the anode humidity decreased in overall cell and the humidity distribution was more uneven in the case that humidification temperature was low (Condition 3). In the case of low humidify temperature, the membrane ionic conductivity decreased by a drop of humidity in overall cell. As a result, the humidity at the upstream area of cathode became low because of decrease of current density and the amount of generated water. On the other hand, the humidity at the downstream area of cathode became high because of increase the amount of water generated by high current density. In Fig. 4(a and d), as compared with Condition 1, it was found that the anode humidity decreased in overall cell in the case of high current density (Condition 4). It was thought that the anode gas became dry because the water transfer to cathode by electro-osmosis increased as current density increased.

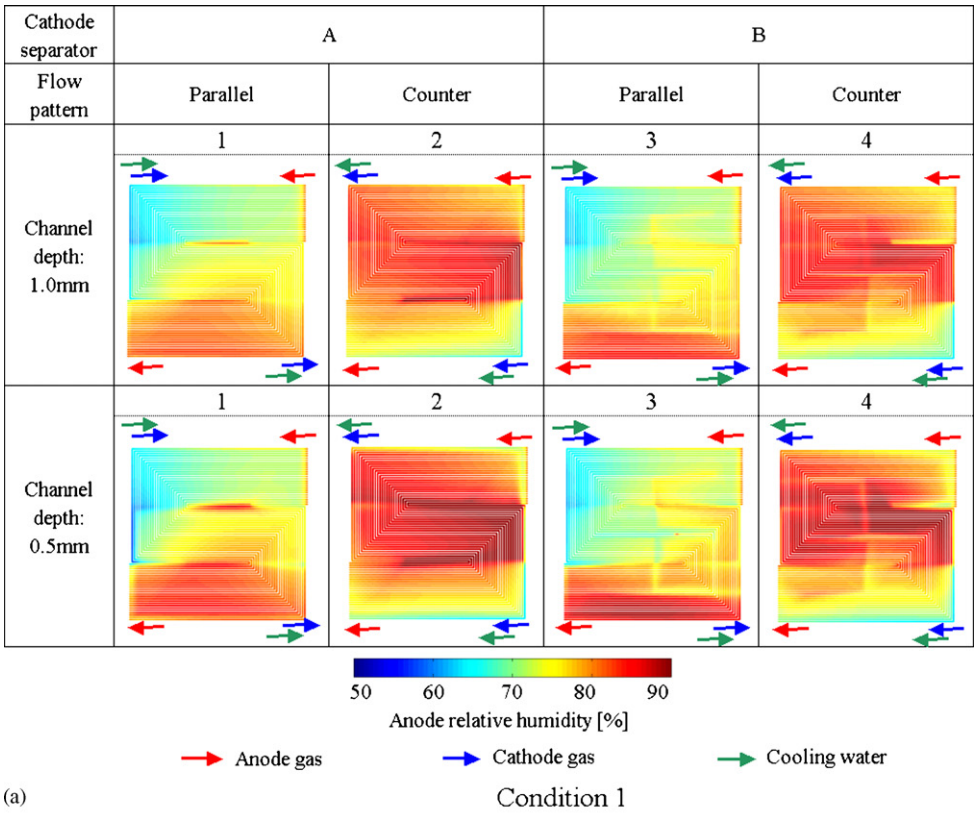

(a) Condition 1

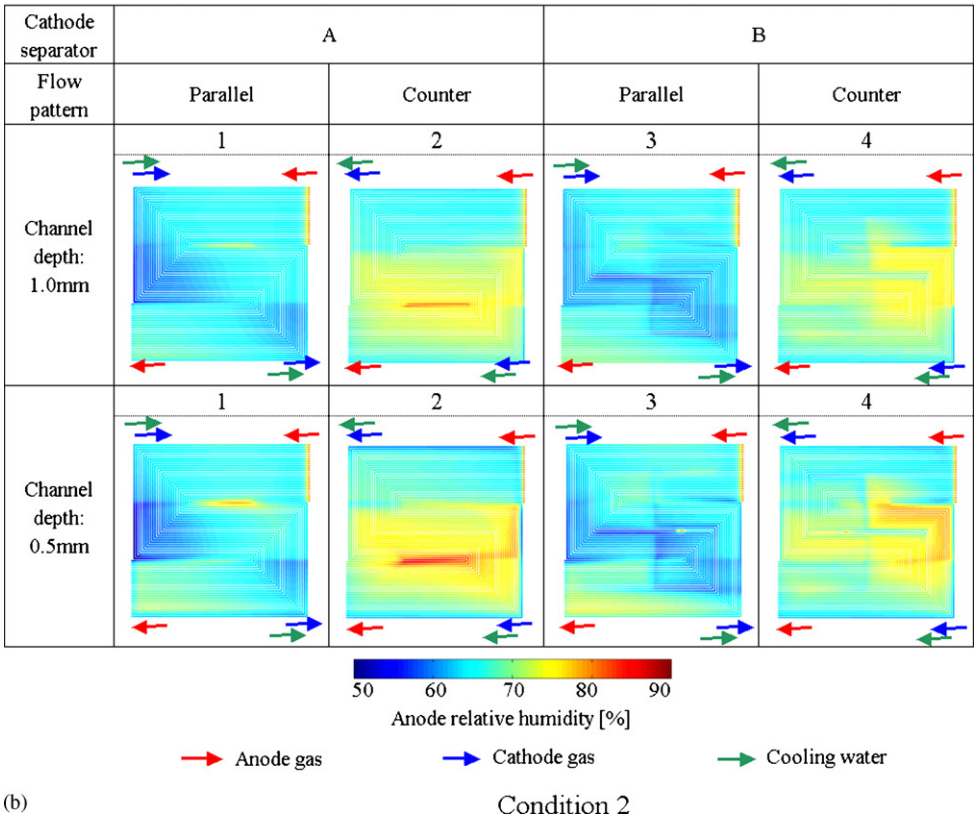

(b) Condition 2

Fig. 4. Calculation results of anode relative humidity distribution under each operating condition.

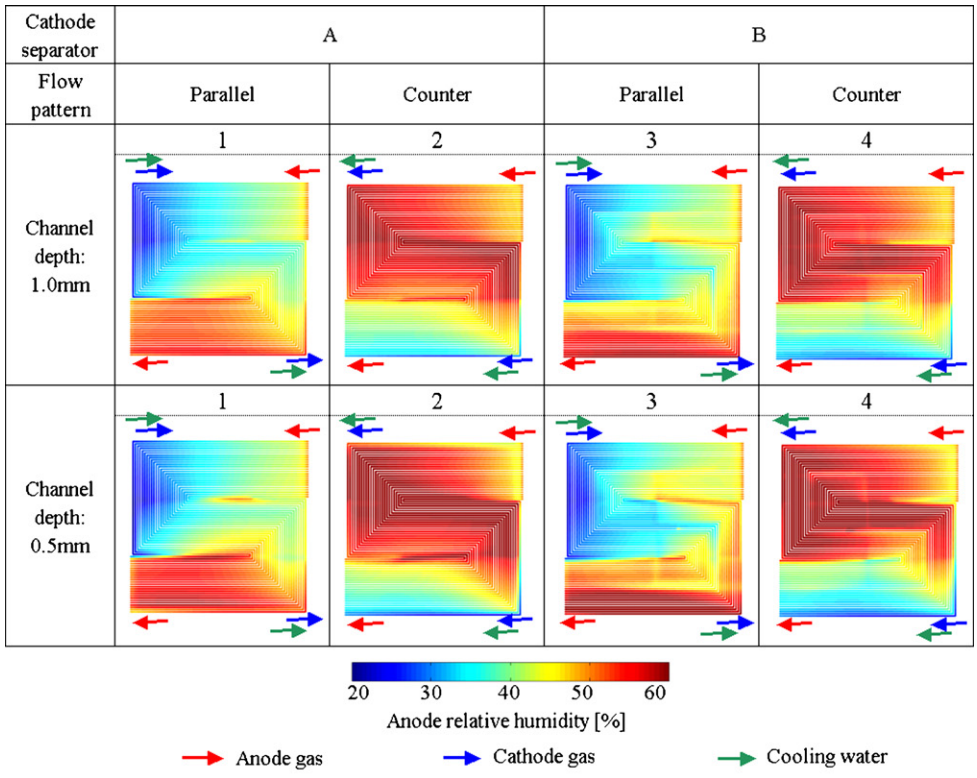

(c) Condition 3

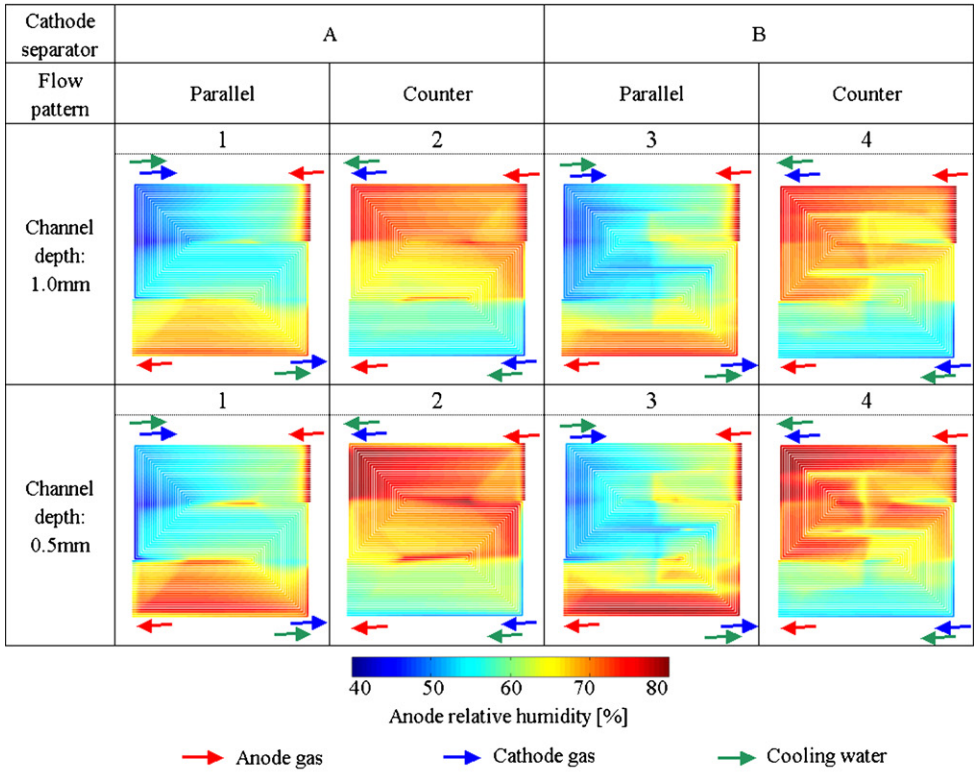

(d) Condition 4

Fig. 4. (*Continued*).

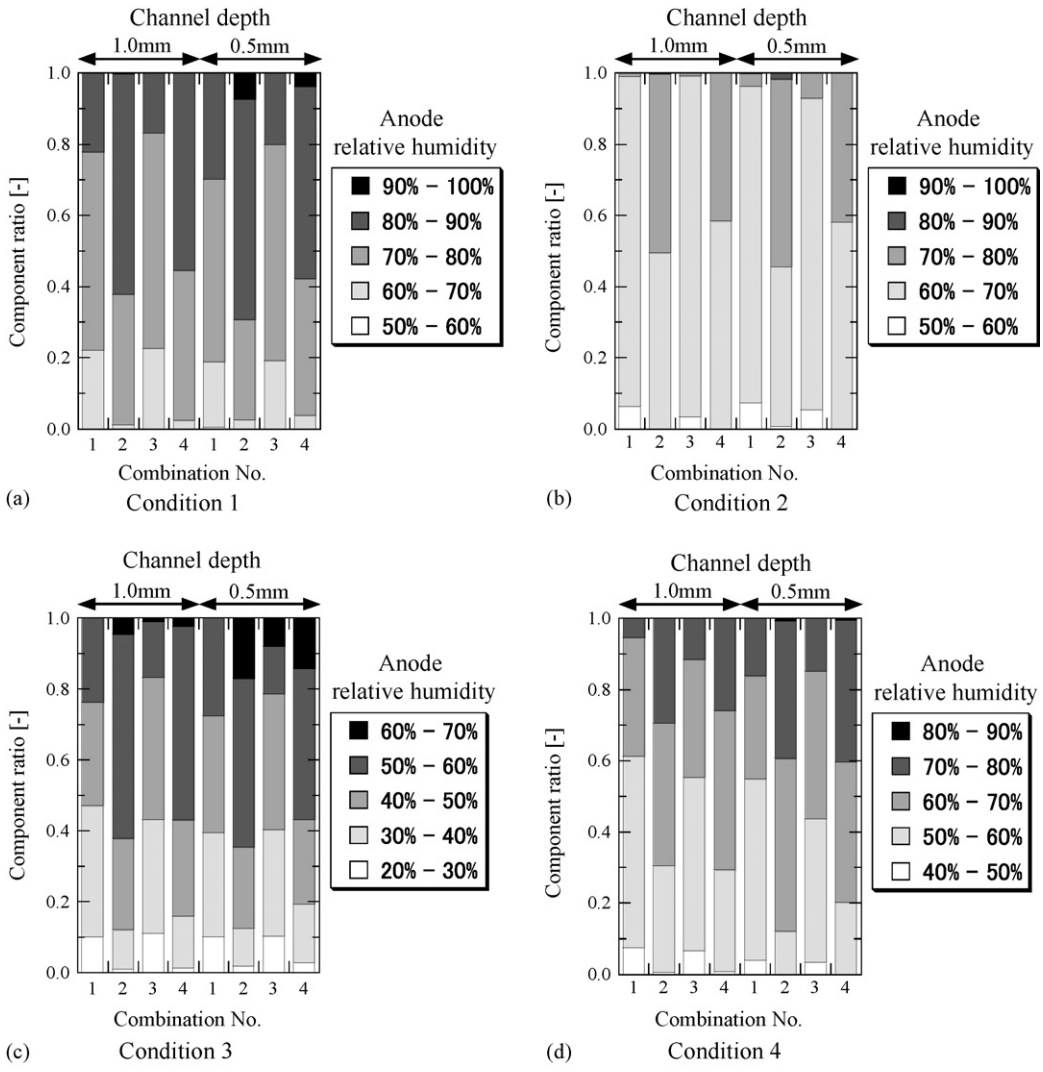

Fig. 5. Component ratio of anode relative humidity distribution under each operating condition.

To investigate the anode relative humidity distribution of Fig. 4 quantitatively, the component ratio of distribution under each operating condition is shown in Fig. 5. In this figure, it was confirmed that the low humidity area of No. 2 was smaller than that of other combinations under each operating condition and that the deep gas channel was effective in uniform humidity distribution because the gas flow rate through GDL was reduced. Consequently, the relative humidity in No. 2 is the highest and the most uniform. The conditions of the examination are as follows; gas flow pattern is counter, the cooling water is synchronized with cathode gas flow and the ordinary serpentine separator with 1.0 mm depth channels is used in anode and cathode sides. And it is expected that this combination is effective in the improvement of cell durability caused by membrane degradation.

However, the flooding problem, which is another factor of degradation, has to be also referred. As the relative humidity of the cathode was higher than that of the anode by generated water, water condensation tends to be occurred on the cathode side. The data of the cathode relative humidity distribution confirms that the cathode local relative humidity exceed 100% under only the one condition in all of 32 operating conditions. Fig. 6 shows the calculation results of cathode relative humidity distribution under the Condition 1 and the cathode relative humidity of this condition is shown in Fig. 6, No. 2. In this figure, it was found that the cathode relative humidity in an overall cell of No. 2 was

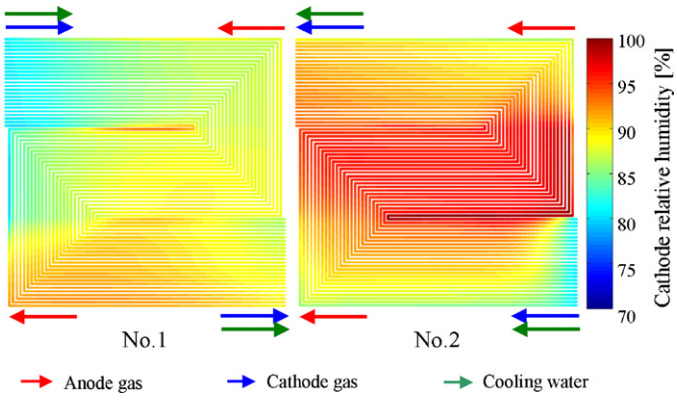

Fig. 6. Calculation results of cathode relative humidity distribution under condition 1.

higher than that of No. 1 and that the highest value in No. 2 was more than 100%. Though the combination of No. 2 is the best to improve the membrane degradation, there is possibility of occurring the flooding which blockade the gas flow and diffusion in No. 2. As a result, the optimum pattern of gas flow has to be decided in consideration of flooding in the cathode. In No. 2, the area which relative humidity exceeded 100% was about 1% of the electrode area. Consequently, in this calculating condition, it is thought that the influence of flooding can be ignored because the excessive condensation is not caused on the cathode side. Similarly, it is thought that such an influence is not occurred on the anode side. Concerning this result, it is necessary to note the following. In this study, the optimal gas shapes of gas channels and the optimal flow pattern for the flooding mean to reduce the extremely high humidity area and to decrease the possibility of condensation of water. However, from the viewpoint of the liquid discharge performance under flooding condition, the optimal shapes of the channels were not considered. Put another way, the purpose of this study is to search the conditions that vapor condensation is not caused by decrease of the high humidity area and it is not to search the conditions that the influence of flooding decreased by improving the water exhausts performance. As the flooding model was not included in this numerical analysis model, the improved model with which the effect of flooding could be examined has to be developed when the internal cell condition is more humid in our future study.

4. Conclusion

In an actual PEFC stack, the relative humidity distribution was calculated on various operating conditions, various shapes of gas channel with PEFC reaction and flow analysis model including the effect of the heat management by cooling water. The optimal shape of separator and the optimal flow pattern of gas and cooling water that make the relative humidity higher and more uniform were examined with this model under each condition. The following results were obtained by these examinations.

(1) The relative humidity at turning areas of channels was higher than that of other areas, because of the effect of gas flow through GDL.
(2) The humidity distribution of counter flow was more uniform than that of parallel flow. As compared with the ordinary serpentine separator, the humidity at turning areas with distributed serpentine separator was lower because the gas flow through GDL was reduced in this separator and the trend became remarkable in the case of shallow channel.
(3) When the cooling water was supplied along the cathode gas flow, the anode humidity at the downstream area of cathode decreased and the humidity distribution was more uniform as the outlet temperature of cooling water was high and this thing was caused by vapor concentration and gas temperature distribution.
(4) As compared with the high humidify temperature, the humidity became low in overall cell in the case of the low humidify temperature and the humidity distribution was more uneven than that of the high humidify temperature because of decrease of membrane ionic conductivity and the change of current density distribution.
(5) When the utilization was constant, the anode humidity decreased in overall cell in the case of high current density. The anode gas became dry because the water transfer to cathode by electro-osmosis increased as current density increased.
(6) The relative humidity is the highest and the most uniform in the following cases: gas flow pattern is counter, the cooling water is synchronized with cathode gas flow and the ordinary serpentine separator with 1.0 mm depth channels is used in both sides. It is expected that this combination is effective in the improvement of cell durability caused by membrane degradation. However, there is possibility of occurring the flooding which blockade the gas flow and the diffusion in this combination as compared with other combinations.

Owing to the numerical analysis model used in this study, it is possible to examine the relative humidity distribution that affects the cell durability caused by membrane degradation and to evaluate the optimal design on various operating conditions and various shape of channel to control humidity distribution. In the author's previous study [11], the validity of this model in a 25 cm^2 cell was confirmed by the generation and flow experiments and it is thought that the results of the calculations with this model is certainly accurate. However, it is needed to experiment the actual size and system of PEFC and to compare the results of the experiments with that of the calculations in order to assure the reliability of this analysis model. In our future study, it is expected that this model will be improved and be compared with experimental results.

Acknowledgement

This research was supported by the research and development of polymer electrolyte fuel cell from the New Energy and Industrial Technology Development Organization (NEDO), Japan.

References

[1] E. Endoh, S. Honmura, S. Terazono, Degradation study of MEA for PEMFC under low humidity conditions, in: Electrochemical Society's Fall Meeting, Honolulu, October, 2004.
[2] C. Zhou, T.A. Zawodzinski, D.A. Schiraldi, Chemical degradation of Nafion™ membranes, in: Electrochemical Society's Fall Meeting, Honolulu, October, 2004.
[3] A.B. LaConti, M. Hamdan, R.C. McDonald, in: W. Vielstich, A. Lamm, H.A. Gasteiger (Eds.), Mechanisms of Membrane Degradation for PEMFCs, Handbook of Fuel Cells: Fundamentals, Technology, and Applications, vol. 3, Wiley, New York, 2003.
[4] A. Hakenjos, H. Muenter, U. Wittstadt, C. Hebling, A PEM fuel cell for combined measurement of current and temperature distribution, and flow field flooding, J. Power Sources 131 (2004) 213–216.
[5] F. Barbir, H. Gorgun, X. Wang, Relationship between pressure drop and cell resistance as a diagnostic tool for PEM fuel cells, J. Power Sources 141 (2005) 96–101.

[6] J. Stumper, M. Löhr, S. Hamada, Diagnostic tools for liquid water in PEM fuel cells, J. Power Sources 143 (2005) 150–157.
[7] P. Quan, B. Zhou, A. Sobiesiak, Z. Liu, Water behavior in serpentine microchannel for proton exchange membrane fuel cell cathode, J. Power Sources 152 (2005) 131–145.
[8] U. Pasaogullari, C.Y. Wang, Two-phase modeling and flooding prediction of polymer electrolyte fuel cells, J. Electrochem. Soc. 152 (2) (2005) A380–A390.
[9] F.Y. Zhang, X.G. Yang, C.Y. Wang, Liquid water removal from a polymer electrolyte fuel cell, J. Electrochem. Soc. 153 (2) (2006) A225–A232.
[10] G. Inoue, T. Yoshimoto, Y. Matsukuma, M. Minemoto, H. Itoh, S. Tsurumaki, Numerical analysis of relative humidity distribution in polymer electrolyte fuel cell stack including cooling water, J. Power Sources (in press).
[11] G. Inoue, Y. Matsukuma, M. Minemoto, Effect of gas channel depth on current density distribution of polymer electrolyte fuel cell by numerical analysis including gas flow through gas diffusion layer, J. Power Sources 157 (2006) 136–152.
[12] G. Inoue, Y. Matsukuma, M. Minemoto, Examination of optimal separator shape of polymer electrolyte fuel cell with numerical analysis including the effect of gas flow through gas diffusion layer, J. Power Sources 157 (2006) 153–165.